Genetics in Medicine (2024) 26, 101081

ELSEVIER

Genetics in Medicine
An Official Journal of the ACMG

www.journals.elsevier.com/genetics-in-medicine

ARTICLE

# Variants in *UBAP1L* lead to autosomal recessive rod-cone and cone-rod dystrophy

Christina Zeitz[1,*], Julien Navarro[1], Leila Azizzadeh Pormehr[1,2], Cécile Méjécase[1,3,4], Luiza M. Neves[1,5], Camille Letellier[1], Christel Condroyer[1], Shahad Albadri[1], Andréa Amprou[1], Aline Antonio[1], Tasnim Ben-Yacoub[1], Juliette Wohlschlegel[1,6], Camille Andrieu[7], Malo Serafini[1], Lorenzo Bianco[1,8], Alessio Antropoli[1,8], Marco Nassisi[1,9], Said El Shamieh[1,10], Sandra Chantot-Bastaraud[11], Saddek Mohand-Saïd[1,7], Vasily Smirnov[1,12], José-Alain Sahel[1,7,13], Filippo Del Bene[1], Isabelle Audo[1,7,*]

ARTICLE INFO

*Article history:*
Received 17 July 2023
Received in revised form
16 January 2024
Accepted 19 January 2024
Available online 28 January 2024

*Keywords:*
Autosomal recessive rod-cone and cone-rod dystrophy
Genome sequencing
Novel gene defect
Retinal organoids
Zebrafish

ABSTRACT

**Purpose:** Progressive inherited retinal degenerations (IRDs) affecting rods and cones are clinically and genetically heterogeneous and can lead to blindness with limited therapeutic options. The major gene defects have been identified in subjects of European and Asian descent with only few reports of North African descent.

**Methods:** Genome, targeted next-generation, and Sanger sequencing was applied to cohort of ~4000 IRDs cases. Expression analyses were performed including Chip-seq database analyses, on human-derived retinal organoids (ROs), retinal pigment epithelium cells, and zebrafish. Variants' pathogenicity was accessed using 3D-modeling and/or ROs.

**Results:** Here, we identified a novel gene defect with three distinct pathogenic variants in *UBAP1L* in 4 independent autosomal recessive IRD cases from Tunisia. *UBAP1L* is expressed in the retinal pigment epithelium and retina, specifically in rods and cones, in line with the phenotype. It encodes Ubiquitin-associated protein 1-like, containing a solenoid of overlapping ubiquitin-associated domain, predicted to interact with ubiquitin. In silico and in vitro studies, including 3D-modeling and ROs revealed that the solenoid of overlapping ubiquitin-associated domain is truncated and thus ubiquitin binding most likely abolished secondary to all variants identified herein.

**Conclusion:** Biallelic *UBAP1L* variants are a novel cause of IRDs, most likely enriched in the North African population.



The Article Publishing Charge (APC) for this article was paid by Sorbonne Université.

Christina Zeitz and Isabelle Audo contributed equally to the article.

Julien Navarro, Leila Azizzadeh Pormehr, Cécile Méjécase, Luiza M. Neves, and Camille Letellier contributed equally to the article.

*Correspondence and requests for materials should be addressed to Christina Zeitz, Department of Genetics, INSERM, UMR_S968, CNRS, UMR_7210, Sorbonne University, Institut de la Vision, 17, rue Moreau, 75012 Paris, France. *Email address:* christina.zeitz@inserm.fr OR Isabelle Audo, Department of Genetics, INSERM, UMR_S968, CNRS, UMR_7210, Sorbonne University, Institut de la Vision, 17, rue Moreau, 75012 Paris, France. *Email address:* isabelle.audo@inserm.fr

Affiliations are at the end of the document.

doi: https://doi.org/10.1016/j.gim.2024.101081

## Introduction

Inherited retinal degenerations (IRDs) are a clinically and genetically heterogeneous group of stationary and progressive diseases, affecting vision.[1] Non-syndromic rod-cone dystrophy (RCD), also called retinitis pigmentosa (RP), is the most common form of IRD with a prevalence of 1:4.000. RCD initially starts with night blindness, secondary to rod photoreceptor dysfunction, followed by peripheral visual-field constriction, and eventually loss of central vision, secondary to cone photoreceptor degeneration.[2] Non-syndromic cone-rod dystrophy (CRD) or cone dystrophy (CD) are less common, with a prevalence of 1:40,000, with primary cone dysfunction and central vision loss,[3] also leading to blindness in most severe cases.[4] RCD and CRD are genetically heterogeneous diseases and have been associated with variants in more than 80 genes[5] (https://web.sph.uth.edu/RetNet/sum-dis.htm). Despite recent advances in high-throughput sequencing, the disease-causing variants are still missing for approximately 20%-40% affected individuals with IRDs.[5] These cases may involve variants in novel disease-associated genes,[6] variants in genes previously associated with a different phenotype,[7,8] overlooked intronic variants,[9,10] structural variants[11] and variants in regulatory regions,[12] which require large cohorts and/or functional analyses for validation.[13] Functional analyses can be based on in vitro or in vivo modeling, including expression and protein immunolocalization studies, minigene approaches, and by the characterization of animal models.[13] More recently, genome sequencing combined with investigations on human induced pluripotent stem cell (hiPSC)-lines differentiated into retinal pigment epithelium (RPE) cells or retinal organoids (ROs) has proven valuable in identifying additional gene defects underlying IRDs.[11,14]

The goal of this work was to identify the gene defect of a subject with autosomal recessive RCD, investigate the candidate gene defect in a cohort of ~4000 index cases with IRDs, validate its relevance using 3D-modeling, and perform expression studies in zebrafish and in RPE cells and ROs differentiated from human iPSC-lines.

## Material and Methods

### Subjects

A cohort of ~4000 cases with IRDs were clinically investigated as previously described.[15] These individuals were recruited at the Reference Center for rare diseases, REFERET, Quinze-Vingts hospital, Paris. The race and ethnicity of the individuals were self-reported, and these French subjects were mainly from European and North African ancestry. Written informed consent for the genetic analysis was obtained from all individuals. All studies were carried out in accordance with the declaration of Helsinki and were approved by a national ethics committee (CPP Ile de France V, Project number 06693, N∘EUDRACT 2006-A00347-44, December 11, 2006).

### Genetic analyses

Total genomic DNA was extracted from whole blood. The affected index individual, CIC03225 of F1362, from a consanguineous Tunisian couple underwent array comparative genomic hybridization (CGH),[6] Sanger sequencing in candidate genes,[16,17] microarray analysis[18] and targeted next generation sequencing (NGS) as previously described.[19,20] Exome sequencing (ES) was performed on the affected index individual CIC03225, the unaffected father CIC03248, the unaffected mother CIC03226, and on 1 unaffected brother CICC03227 of F1362 (Figure 1A) as described before.[23] Genome sequencing (GS) was done on the affected index individual CIC03225 and all available family members (Figure 1A). Paired-end sequencing (2 * 150b) was performed by a company (Integragen) using a NovaSeq600 with a coverage of 30X. Burrows-Wheeler Aligner (BWA) tool was used to map the reads to the Human genome build (hg38). Single nucleotide variants and small indels calling was performed via Broad Institute's GATK Haplotype Caller GVCF tool (GATK 3.8.1) and the Ensembl's VEP (Variant Effect Predictor, release VEP 95.1) program processed the variants for further annotation. Variants were prioritized on the basis of a minor allele frequency (MAF) $\leq$ 0.0005 in the genome Aggregation Database (http://www.gnomad-sg.org/ gnomAD v3.1.1), representing insertions or deletions (InDels), nonsense, missense, splice site variants and assessed for their pathogenicity through bioinformatic tools, including Polymorphism Phenotyping v2 (PolyPhen2, http://genetics.bwh.harvard.edu/pph2/), Sorting Intolerant From Tolerant (SIFT, http://sift.jcvi.org/), MutationTaster (http://www.mutationtaster.org/), amino acid conservation across species with UCSC Genome Browser (http://ge-nome.ucsc.edu/index.html; Human GRCh38/hg38 Assembly), SpliceAI,[24] and Pangolin,[25] similarly as performed before.[23] Further prioritization was done by keeping variants present in regions of homozygosity (ROHs) unique to the affected member. The ROHs were established by doing homozygosity mapping using a program (AutoMap 1.2)[26] on all family members, then discarding regions shared by affected and unaffected members. Direct sanger sequencing on genomic DNA from whole blood from all available family members of F1362 (Figure 1A) was used to validate putative disease-causing variants or to perform cosegregation analyses. To detect putative copy-number variants in affected cases with monoallelic variants in the candidate gene, quantitative PCR experiments using primers covering all exons and a kit (SYBR Green Real-Time PCR Master Mixes, Applied Biosystems, Thermo Fisher) was performed similarly as previously.[6] The conditions are available on request.

Subsequently, the candidate gene was screened in affected individuals from our French cohort mainly of

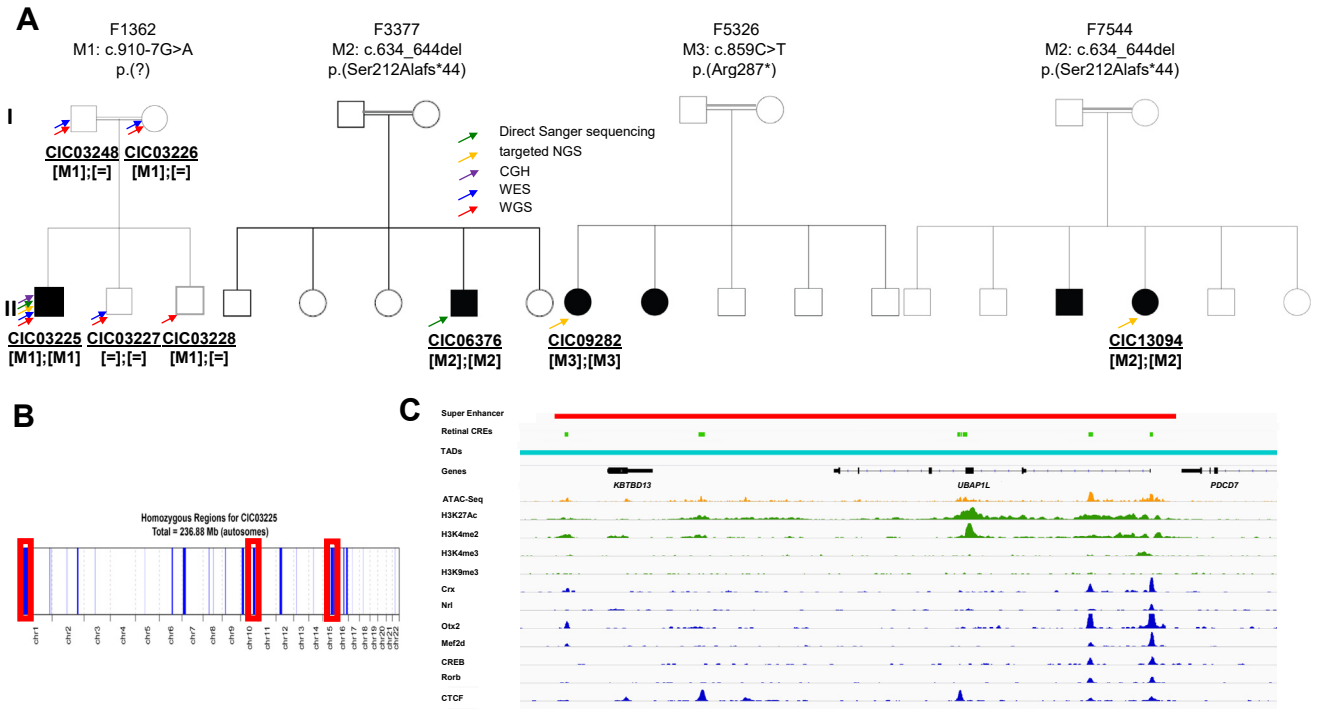


**Figure 1 Families with autosomal recessive RCD and CRD/CD and pathogenic variants in *UBAP1L*.** A. Pedigrees of the 4 families (F1362, F3377, F5326, and F7544) with variants in *UBAP1L* cosegregating with the phenotype in all available family members. The arrows indicate the genetic screening performed on each subject. DNA from the family members of family F3377, F5326, and F7544 were unavailable, but because of the reported consanguinity, we presumed that M2 and M3 occurred homozygous in the affected index cases. B. Homozygosity mapping using WGS data identified 3 large (>20 Mb) homozygous regions in the affected index individual CIC03225 of F1362 with sizes of 27.7, 20.9, and 25.8 Mb mapping to chromosome 1, 10, and 15, respectively. C. Super Enhancer (red), retinal *cis*-regulatory elements (light green), topologically associated domain (teal), chromatin accessibility (orange), histone modifications (green), and transcription factors residency (blue) for the *UBAP1L* locus. Chromatin accessibility has been defined by ATAC-seq from post-mortem adult human retina. Histone modifications and transcription factor residency have been defined by ChIP-seq from post-mortem adult human retina. Super enhancer and retinal *cis*-regulator elements have been calculated from previously described experimental data.[21,22]

European and North African descendants, by direct Sanger sequencing (conditions will be delivered on request) and/or by targeted NGS, similarly as previously described.

## Fibroblasts reprogramming into iPSCs and differentiation into RPE cells and into ROs

Human dermal fibroblasts from the affected index case CIC03225 and unaffected brother CICC03228 of F1362 were obtained after informed consent at the Quinze-Vingts hospital from a skin biopsy and expanded as described before (Ethical approval: Comité de Protection des Personnes Ile de France V [2012-A01333-40; P12-02] and the ANSM [B121362-32]).[27] Subsequently, they were reprogrammed into iPSCs using reprogramming vectors (CytoTune Sendai OCT3/4, SOX2, CMYC, and KLF4, Thermo Fisher Scientific).[27] The iPSC colonies were obtained and expanded under feeder free conditions.[28] Pluripotency was tested as performed before, using a Scorecard technique (Thermo Fisher Scientific).[29] For genomic integrity and concordance with parental fibroblasts, the samples were analyzed by single nucleotide variant arrays using Illumina InfiniumCore-24 technique (Illumina) at Integragen.[29] Subsequently, iPSCs were differentiated in ROs and RPE cells.[28]

## Expression analysis

The expression of the *UBAP1L* (HGNC:40028) was investigated using publicly and in-house available database (https://www.proteinatlas.org/search/UBAP1L and https://singlecell.broadinstitute.org/single_cell/study/SCP484/nucseq-from-human-control-eyes-scrnaseq[30]) as previously described.[23] Subsequently, its expression was experimentally verified by RT-PCR experiments using commercially available cDNA of different human tissues (Clontech), cDNA from human fibroblasts, human-induced iPSCs, ROs, and RPE cells of an unaffected individual. A detailed protocol can be provided on request.

## Splice defect investigation on ROs

The consequence of the homozygous NM_001163 692.2:c.910-7G>A variant on splicing of *UBAP1L* for the affected index individual CIC03225 and his heterozygous unaffected brother CIC03228 of family F1362 was

investigated by RT-PCR experiments applied to ROs of the respective individuals. Forward and reverse oligonucleotides in exons 4 and 5, and 6 amplified transcripts, including the NM_001163692.2:c.910-7G>A variant, which was present in intron 4 of *UBAP1L*. The respective products were Sanger sequenced. A detailed protocol can be provided on request.

### Zebrafish strain and husbandry

Zebrafish (Danio rerio) were bred and maintained at the aquarium of the Institut de la Vision, Paris, France as described before.[31] Zebrafish were maintained at 28 °C on a 14-hour light/10-hour dark cycle. All animal procedures were performed in accordance with French and European Union animal welfare guidelines with protocols approved by committee on ethics of animal experimentation of Sorbonne Université (APAFIS#21323-2019062416186 982).

### Zebrafish RNA in situ hybridization and hybridization chain reaction (HCR) analyses

The 5′- CTGCAGGAAACTGAGTATGTGTTC-3′ fw and 5′-CCAAGCTTCTAATACGACTCACTATAGGGAGAT TCATTAAACTGAGCCAGAAGATGC-3′ T7-rv primer-set was used to amplify *ubap1lb* transcript and the digoxigenin-labeled riboprobe were prepared as recommended by the manufacturer instructions (Roche). Single whole-mount in situ hybridization of the zebrafish *ubap1lb* gene (XM_002666995, NCBI accession number) was carried out as previously described.[32] The *ubap1lb* riboprobe was labeled with digoxigenin-UTP (Roche). Hybridization with the probe was carried overnight at 68 °C. Anti-DIG primary antibody coupled to alkaline phosphatase (Roche) and NBT-BCIP (Roche) were used for signal detection. Embryos, 5 days after fertilization stained with NBT/BCIP were mounted in 87% glycerol on microscope slides and imaged with a microscope (Leica MZ10F). For vibratome sections, whole-mount embryos were washed twice in 1× PBS/0.1% Tween-20 (PBS-Tw) solution. The samples were embedded in gelatin/albumin with 4% of glutaraldehyde and sectioned (20 mm) on a VT1000 S vibrating blade microtome (Leica). Sections were mounted In Fluoromount Aqueous Mounting Medium (Sigma, Merck kGaA).

The HCR procedure was performed following the manufacturer instruction (Molecular Instruments) and the *ubap1lb* probe designed. Labeled embryos were embedded and mounted on 100 × 15 mm glass bottom dishes in 1% low melting agarose and *ubap1lb* HCR probe signal was acquired using a confocal microscope (LSM 900, Zeiss) using a 40× water immersion objective. Software were used for image analyses (Imaris Viewer 10.0, Oxford Instruments Group) and image processing (Adobe Photoshop, Adobe Illustrator).

### 3D-modeling

The wild-type 3D structure of UBAP1L (UniprotKB: F5GYI3) was downloaded from the official AlphaFold database: https://alphafold.ebi.ac.uk/. For the mutated proteins the AlphaFold (version 2.3.2) protein folding prediction program using the monomer model with default settings was used.[33]

## Results

### Phenotypic characteristics of affected individuals

At presentation, CIC03225, F1362, was a 23-year-old male subject who complained of night blindness and progressive visual-field constriction since he was 20 years old. He was the oldest son from a consanguineous Tunisian couple (Figure 1A). Best corrected visual acuity (BCVA) was 20/32 for both eyes (BE) with −7 diopter optical correction. He had a tritan defect on color-vision testing (Lanthony's 15 desaturated Hue). Kinetic visual-field assessment showed the presence of paracentral scotomas. Full field electroretinogram (ff-ERG) was undetectable. Retinal imaging revealed typical signs of RCD with macular atrophy in BE (Figure 2). CIC06376, F3377 was a 50-year-old Tunisian male from a consanguineous union (Figure 1A) with a clinical diagnosis of CRD. BCVA was 20/200 in the right eye (RE) and 20/50 in the left eye (LE) with no specific optical correction. Kinetic visual-field testing revealed the presence of a central scotoma in BE. Ff-ERG showed only residual responses under scotopic conditions confirming the severe cone-rod dysfunction. Retinal imaging displayed a pale optic disc, narrowed retinal vessels and atrophic changes of the posterior pole and the inferior retina in BE (Figure 2). CIC09282, F5326 was a 55-year-old Tunisian woman, from a consanguineous couple (Figure 1A). She was referred to the rare disease center with a presumed diagnosis of Stargardt disease. BCVA was 20/500 with −0.50(−2.25)15° in the RE and 20/400 with −0.50(−1.50)160° in the LE. Color-vision testing revealed complete dyschromatopsia. Kinetic visual-field assessment showed severe constriction in BE. Ff-ERG revealed only residual responses under scotopic conditions consistent with severe cone-rod dysfunction. Retinal imaging revealed a pale optic disc, narrowed retinal vessels, and atrophic changes predominant at the posterior pole in BE (Figure 2). CIC13094, F7544 was a 50-year-old female from a consanguineous Tunisian couple (Figure 1A) when she was first assessed at the rare disease center. She has been complaining about night blindness since teenaged. BCVA was 20/160 with −1.25(2)175° in the RE and 20/800 with −0.50(−2.25)175° in the LE. Kinetic visual-field testing revealed a central scotoma for BE. Again, ff-ERG

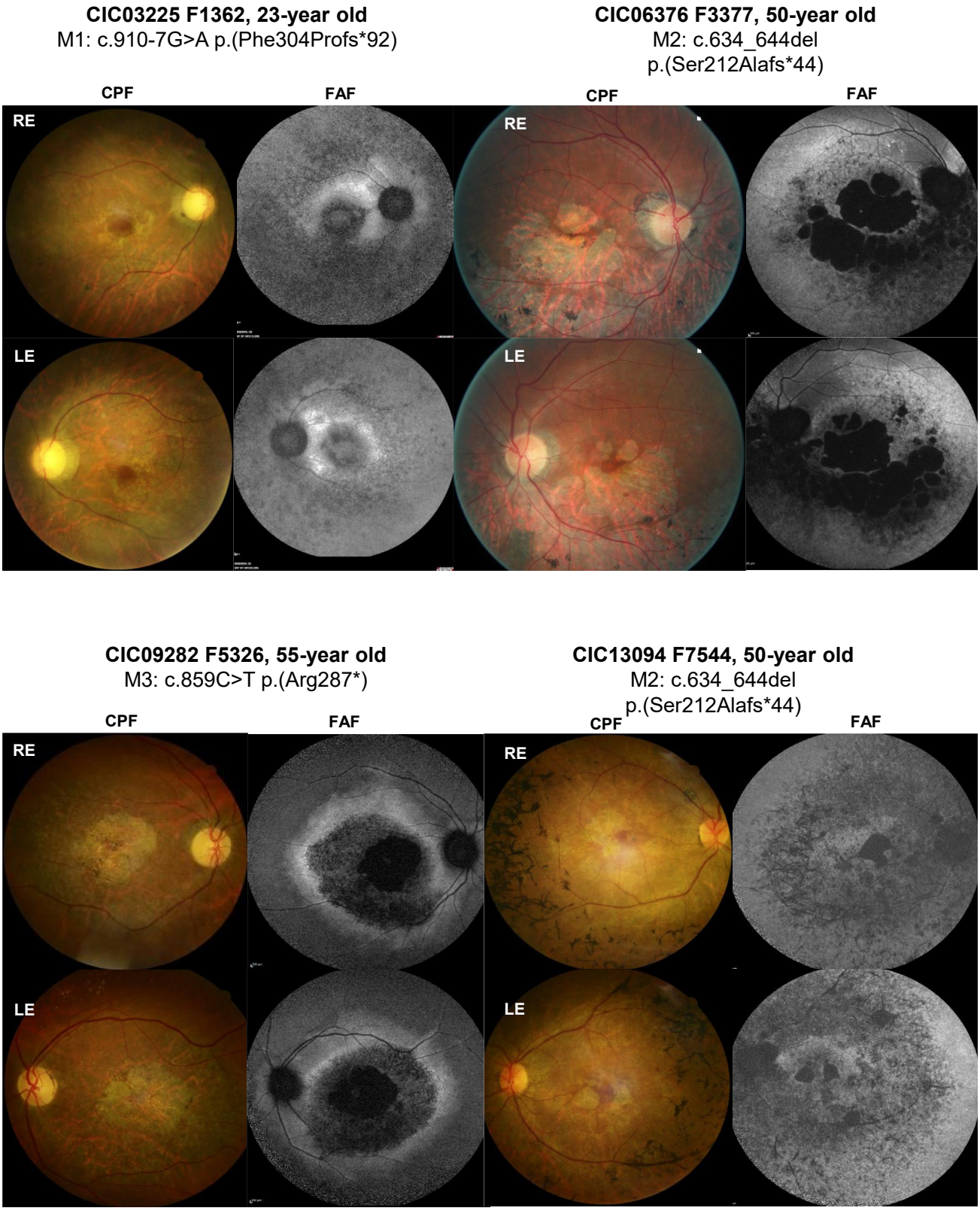


**Figure 2 Retinal images of index cases carrying homozygous variants in *UBAP1L* (CIC03225, CIC06376, CIC09282, and CIC13094).** Color fundus photographs (CFP) and fundus autofluorescence imaging (FAF) of the right and left eye (RE and LE, respectively). CIC03225's fundus examination revealed typical signs of RCD with pale optic discs, narrowed retinal vessels, and central macular atrophy and a loss of autofluorescence in the periphery, as well as in the macular region. CIC06376 showed central macular atrophy expending into the mid periphery predominantly in the inferior sector and a loss of autofluorescence in the atrophic areas surrounded by an area of heterogeneous autofluorescence expanding in the mid periphery. CIC09282 had pale optic discs, narrowed retinal vessels, and atrophic changes in the macular area with a loss of central autofluorescence surrounded by a ring of increased autofluorescence. CIC13094 had central macular atrophy and speckled appearance of autofluorescence at the posterior pole and mid periphery.

responses were only observed under scotopic conditions, indicating severe cone-rod dysfunction. Retinal imaging revealed atrophic changes in the posterior pole and mid periphery in BE (Figure 2). The summary of the clinical data of all individuals with *UBAP1L* variants and a figure showing a normal fundus upon photography and autofluorescence imaging can be found in the Supplemental Table and Figure.

## Identification of 3 *UBAP1L* variants in 4 cases from 4 unrelated families

The genetic causes of RCD for the affected index, CIC03225 (F1362, Figure 1A), from a consanguineous Tunisian couple remained unsolved despite conducting Sanger sequencing of candidate genes implicated in RCD (eg, Audo et al[16,17]), microarray analysis,[18] targeted NGS using a panel of 123 genes or candidate genes implicated in IRDs[19] and ES.[23] Similarly, the search for structural variations using ES raw data did not reveal any candidate copy-number variation. However, array CGH and homozygosity mapping using WGS data identified 3 large (>20 Mb) homozygous regions in the affected index with sizes of 27.7, 20.9, and 25.8 Mb mapping on chromosome 1, 10, and 15, respectively (Figure 1B). Applying stringent filtering, we identified a homozygous variant in chromosome 15: NM_0011 63692.2:c.910-7G>A (allele frequency in gnomAD: 1.64e-4, with no homozygous appearance) in a gene, *UBAP1L* within the 25.8 Mb homozygous region on chromosome 15q22.31 in this affected individual. Notably, this gene was absent in a database, which associates genes with IRDs: https://sph.uth.edu/retnet/sym-dis.htm. This variant co-segregated with the phenotype in this family (Figure 1A) and was predicted to create a new AG acceptor site at position NM_00 1163692.2:c.910-5, which would lead to an altered longer protein p.(Phe304Profs*92). Alternatively, nonsense-mediated mRNA decay could take place. Previous ES analysis had overlooked this variant because it was not affecting a canonical splice site. A heterozygous *PROM1* (HGNC:9454) variant, NM_006017.3:c.314A>G p.(Tyr105Cys) was considered as not disease causing because the unaffected mother, CIC03226, and the unaffected brother, CIC03228, were also heterozygous for this variant. Interestingly, *UBAP1L* was one of 19 potential candidate genes previously listed in a genetically unsolved RP case originating from South Asia.[34] Noteworthy, *UBAP1L* lies within a super enhancer (SE) region, which was identified by chromatin immunoprecipitation sequencing (ChIP-seq) performed on post-mortem adult human retinas.[21,22] This region contains a cluster of retinal *cis*-regulatory elements (CREs). CREs are characterized by a high density of histone modifications associated with promoters and active or poised enhancers. Specifically, the presence of histone modification H3K27Ac, commonly associated with active enhancers is observed in these CREs. In additions, the presence of ATAC-seq signals indicate a high-chromatin accessibility in these regions (Figure 1C[21,22]). These elements supported *UBAP1L* as a strong candidate gene underlying IRDs.

Subsequently, Sanger sequencing of our genetically unresolved French cohort mainly of European and North African descendants, revealed another affected individual (CIC06376, F3377) from a consanguineous Tunisian couple with a presumably homozygous deletion, NM_001163692.2:c.634_644del (allele frequency in gnomAD: 2.64e-5, with no homozygous appearance) in *UBAP1L*. This deletion was predicted to result in a premature stop codon, p.(Ser212Alafs*44) or mRNA decay (Figure 1A). Similarly, an updated targeted NGS, including recent candidate genes, identified a third case (CIC13094, F7544) from a consanguineous Tunisian couple harboring the same variant (Figure 1A). This patient revealed also a most likely homozygous *RP1L1* (HGNC:15946) variant, NM_178857.6:c.92C>T p.(Thr31Met), which was predicted to be benign. In addition, using this method, a presumably homozygous nonsense variant, NM_001163692.2:c.859C>T (allele frequency in gnomAD: 3.29e-5, with no homozygous appearance), in *UBAP1L*, predicted to lead to a premature stop codon, p.(Arg287*) or nonsense-mediated mRNA decay was identified in a fourth family (CIC09282, F5326) from another consanguineous Tunisian couple (Figure 1A). This patient revealed also a heterozygous *GUCY2D* (HGNC:4689) variant, NM_000180.4:c.1984G>A p.(Val662Met), which was predicted to be benign.

All 4 affected index individuals with *UBAP1L* variants identified herein reported consanguinity among their parents and were from Tunisian couples. This was further confirmed by homozygosity mapping analysis in F1362, which could be done with available WGS data, showing multiple homozygous regions in the affected index case, which were absent in the unaffected family members (Figure 1B). For F5326, homozygosity mapping using available targeted NGS data also revealed a 35 Mb homozygous region encompassing *UBAP1L*. Furthermore, none of the sequenced polymorphisms in the coding regions of *UBAP1L* were found to be heterozygous in F3377 and F7544. These findings collectively support the notion that the gene defect in *UBAP1L* is indeed located within a homozygous region, consistent with the consanguinity in all families.

## *UBAP1L* is expressed in the brain, RPE cells, in the retina and more precisely in rod and cone photoreceptors

Transcriptomic databases reported that human *UBAP1L* is expressed in the brain, the eye and more specifically in RPE cells as well as in rod and cone photoreceptors[30] (Figure 3A). These data were confirmed by RT-PCR experiments (Figure 3B). *UBAP1L* was found to be expressed in human universal embryonal tissue and lung, but more importantly in brain, retina, fibroblasts, hiPSCs, ROs, and RPE cells differentiated from iPSCs from an unaffected individual (Figure 3B). In human universal embryonal tissue

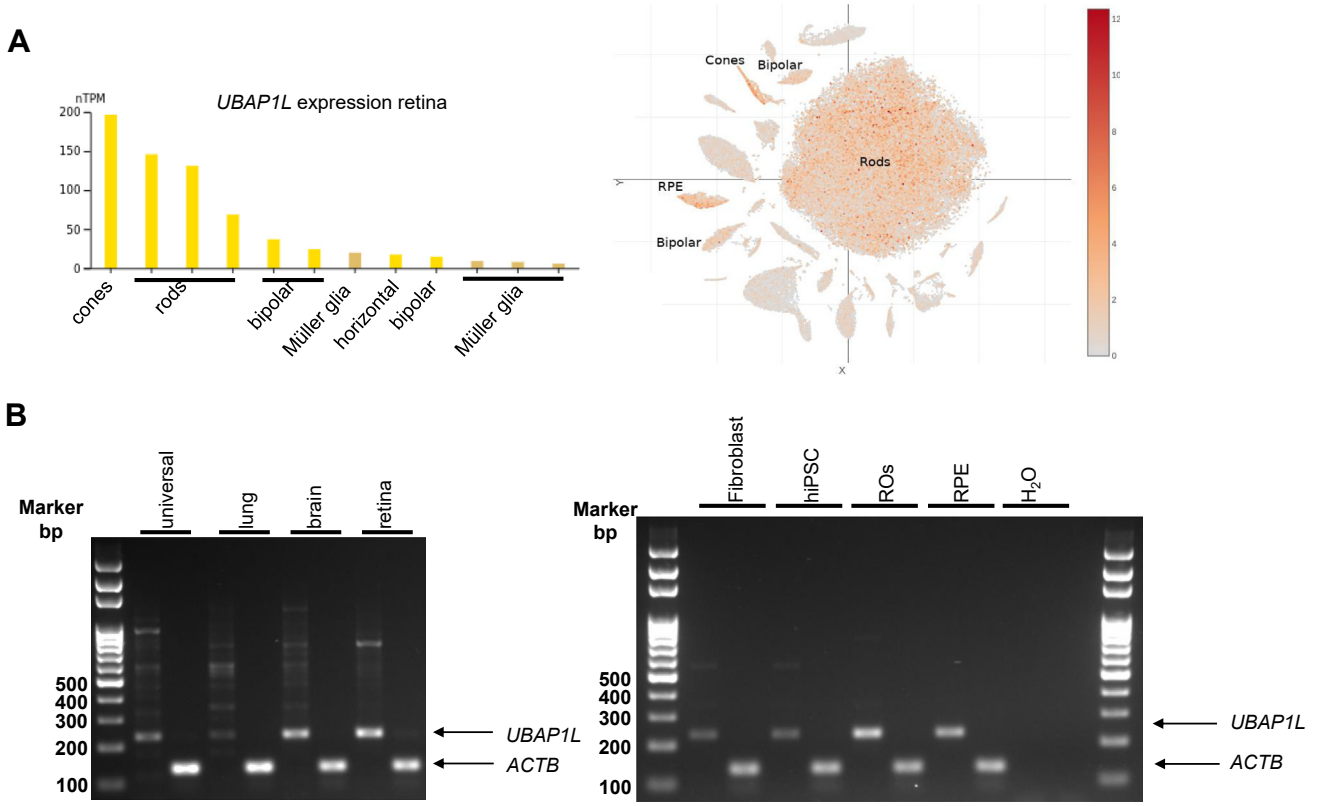


**Figure 3 Expression analysis of *UBAP1L* mRNA in human tissues by RT-PCR experiments.** A. Expression analyses using databases revealed that the human *UBAP1L* gene is expressed in the eye and more specifically in RPE cells and rod and cone photoreceptors with a low expression in bipolar cells. B. *UBAP1L* was found to be expressed in human universal embryonal tissue and lung but, more importantly, in brain, retina, fibroblasts, hiPSCs, retinal organoids (ROs), and RPE cells differentiated from hiPSCs. Other unspecific transcripts appeared in universal tissue and lung.

and lung other unspecific transcripts appeared (Figure 3B). In silico analysis revealed 2 isoforms of *UBAPL1* in the zebrafish, named *ubap1la* and *ubap1lb*. We decided to investigate the expression of these 2 genes during normal zebrafish development. Notably, *ubap1lb* exhibited a remarkably distinct expression pattern in zebrafish larvae at 3 and 5 days after fertilization. In situ hybridization and HCR on zebrafish embryos revealed that the *ubap1lb* isoform is specifically expressed in the retina, and more specifically in rod and cone photoreceptors (Figure 4). This gave further evidence for a role of UBAP1L during normal retinal development and its potential alteration in the pathological retina.

## The NM_001163692.2:c.910-7G>A variant leads to missplicing of *UBAP1L* in ROs

To investigate if the NM_001163692.2:c.910-7G>A, located in intron 4, of *UBAP1L*, indeed, leads to an altered longer protein p.(Phe304Profs*92) or to nonsense-mediated mRNA decay, RT-PCR experiments were performed on ROs at 150 days of the affected individual CIC03225 and his unaffected heterozygous brother, CIC03228 of F1326. These revealed in ROs of the patient the insertion of 5 nucleotides (GCCCA), whereas in ROs of the unaffected brother, both the reference and mutated mRNA sequence were present, as confirmed by Sanger sequencing (Figure 5). These findings confirmed the in silico prediction for missplicing associated with the NM_001163692.2:c.910-7G>A variant in *UBAP1L* leading most likely to a longer protein p.(Phe304Profs*92). Other bands occurring in the unaffected heterozygous brother were not investigated in detail.

## In silico predictions and in vitro functional characterization of *UBAP1L* variants

*UBAP1L* (NM_001163692.2) containing 6 exons codes for Ubiquitin-associated protein 1-like comprising 381 amino acids. The open reading frame starts in exon 2 and ends in exon 6 (Figure 6A). The protein contains a solenoid of overlapping ubiquitin-associated (UBA) domains (SOUBA), which was shown to interact with ubiquitin in UBAP1.[35] The SOUBA domain starts at amino acid residue Ser269 and ends at the C terminus. It is composed of 3 overlapping UBAs forming each 3 α-helices (Figure 6B). Thus, the SOUBA domain is formed by 7 α-helices (α1-α7), as shown in the 3D model (Figure 6C, wild type).

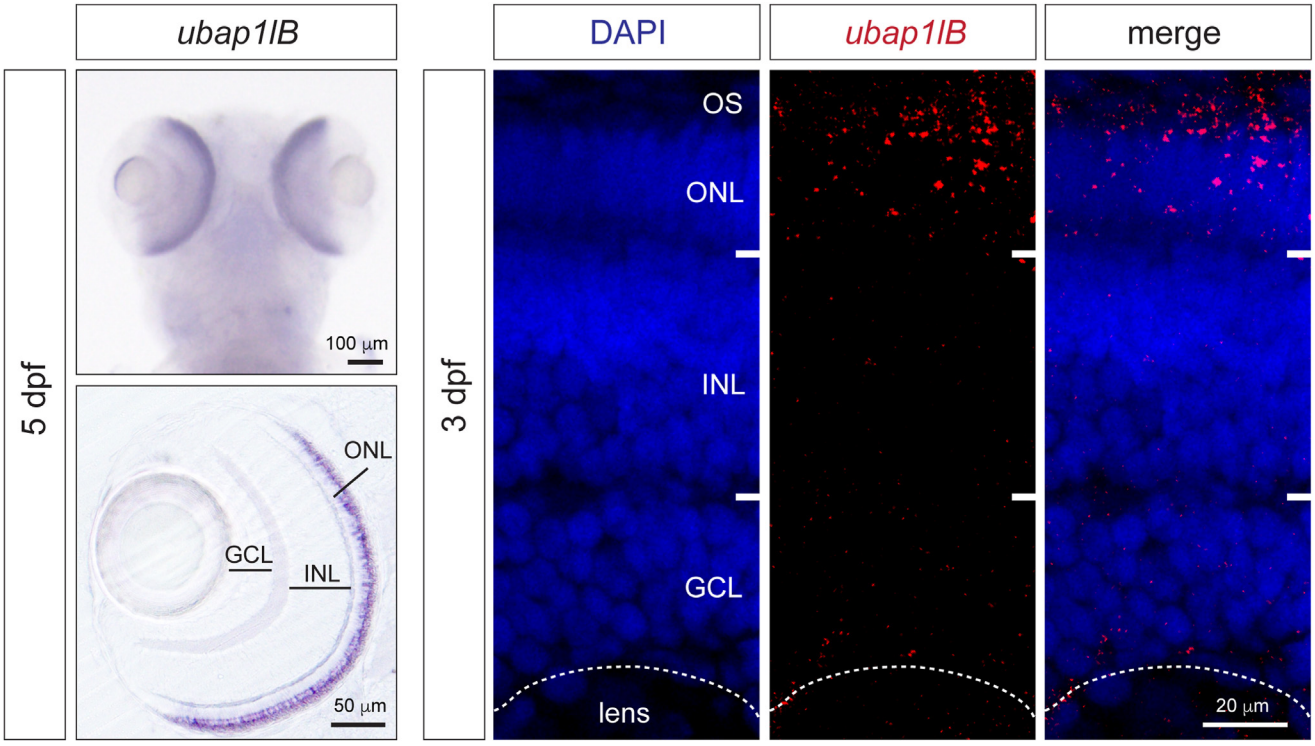


**Figure 4 Expression analysis of *ubap1l* in zebrafish.** In situ hybridization for *ubap1lb* in zebrafish larvae 5 days after fertilization (left). The dorsal view is on the top and retina vibratome section is on the bottom. Expression can be detected in the retina in the photoreceptor layer. On the right, fluorescent HCR in situ hybridization on 3 days after fertilization larvae confirms *ubap1lb* mRNA expression in the OS and ONL where photoreceptors are located. ONL, outer nuclear layer; INL, inner nuclear layer; GCL, Ganglion cell layer; OS, outer segment.

The 3 variants in *UBAP1L* identified in this study could all affect the SOUBA domain (Figure 6). The NM_00 1163692.2:c.634_644del, located in exon 3 that leads to the frameshift p.(Ser212Alafs*44) occurs upstream of the SOUBA domain (Figure 6B). Therefore, none of the 7 α-helices would remain, meaning that there is no UBA left to bind ubiquitin (Figure 6C). Similarly, the NM_001163692.2:c.859C>T, located in exon 4 that leads to the premature stop codon p.(Arg287*), occurs within the SOUBA domain. Therefore, only α1 and a small part of α2 remain (Figure 6C), which severely alter the capabilities of the protein to bind ubiquitin. However, both variants may most likely cause nonsense-mediated mRNA decay, leading to complete loss of function. Previously, another variant in *UBAP1L*,

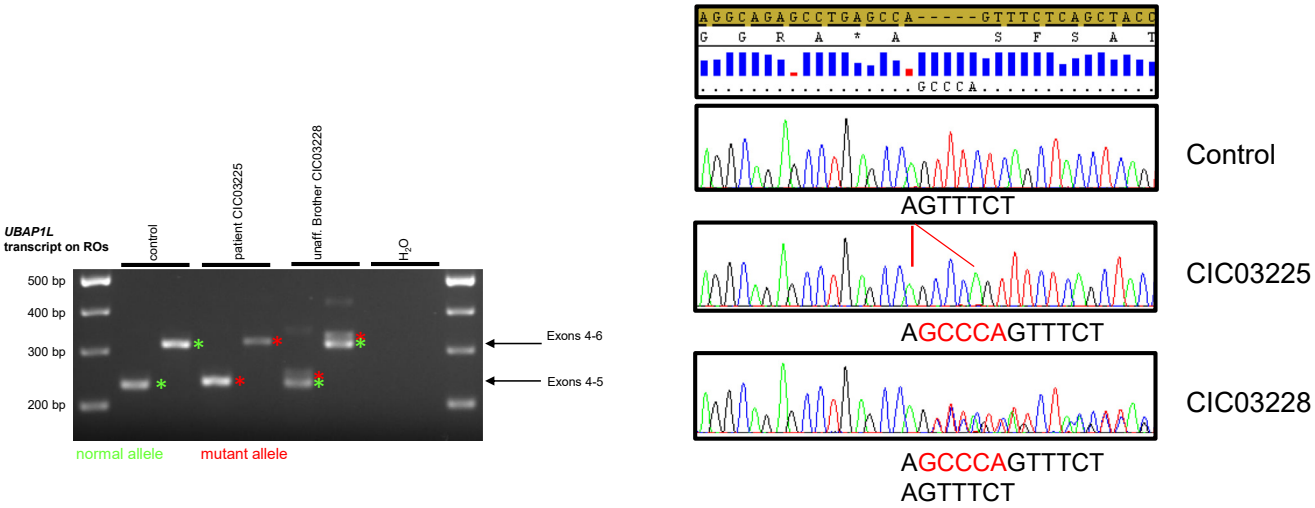


**Figure 5 Mis-splicing in ROs of an affected individual lead to a longer protein.** RT-PCR experiments performed on ROs at 150 days from the affected individual, CIC03225, revealed a 5-nucleotide insertion, whereas the unaffected heterozygous brother, CIC03228, revealed both the 5-nucleotide insertion and the reference sequence on transcript level, as confirmed by Sanger sequencing. These findings confirmed the in silico prediction for mis-splicing of the c.910-7G>A in *UBAP1L*, leading most likely to a longer abnormal protein p.(Phe304Profs*92).

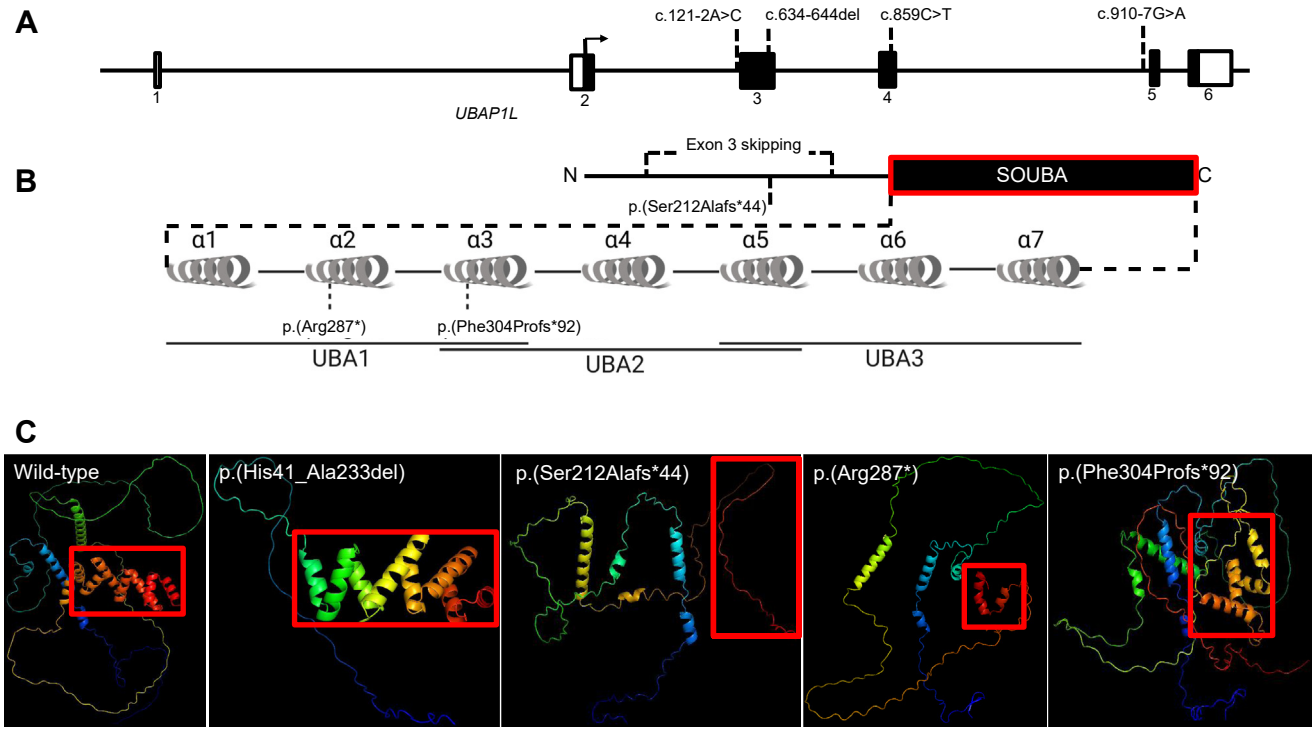


**Figure 6 Gene structure, prediction of domains and 3D-modeling of the unaffected and altered UBAP1L protein.** A. Schematic representation of *UBAP1L* gene structure with the positions of identified variants. B. Schematic representation of UBAP1L protein structure with the positions of identified variants. The SOUBA domain structure is detailed showing the composition of UBAs and α-helices. C. AlphaFold 3D structure predictions of UBAP1L wild-type (UniprotKB: F5GYI3), p.(His41_Ala233del), p.(Ser212Alafs*44), p.(Arg287*), and p.(Phe304Profs*92). The color scheme is a gradient that goes from N terminus (blue) to C terminus (red).

NM_001163692.2:c.121-2A>C (Figure 6A) was described as a possible cause for RP.[34] It was predicted to lead to exon 3 skipping and an in-frame deletion, p.(His41_Ala233del) (Figure 6B), which would not affect the SOUBA domain but delete a significant proportion of the coding sequence amino, which will most likely also affect the protein function (Figure 6C). The NM_001163692.2:c.910-7G>A, located in intron 4 was predicted to affect splicing, with a delta score of 0.99 by SpliceAI and 0.84 by Pangolin leading to an altered longer protein, p.(Phe304Profs*92). Indeed, our studies performed on ROs confirmed the missplicing (Figure 5). The frameshift starts in exon 5, which also codes for the SOUBA domain. Therefore, if the variant leads to an altered protein product, only α1, α2, and a small part of α3 would remain, severely altering the capabilities of the protein to bind ubiquitin (Figure 6C). Therefore, we think that all variants identified herein are predicted to lead to a highly modified protein, which will be unable to bind ubiquitin.

## Discussion

Variants implicated in progressive non-syndromic RCD or CRD affect genes expressed in photoreceptors and/or RPE, and they code for proteins involved in different cellular functions, including phototransduction, cellular differentiation, structure and maintenance, retinal metabolism and splicing.[4] To date variants in more than 80 genes (https://web.sph.uth.edu/RetNet/sum-dis.htm) can lead to these conditions.[5] With the new advent of NGS, novel gene defects were rapidly discovered. It is much likely that all the major gene defects underlying IRDs have now been reported. As shown in our center, up to 80% of the cases can be solved by a combination of Sanger and targeted NGS. However, it remains challenging to determine the genetic cause for the remaining 20% of cases, even when using comprehensive ES and GS methods. Novel gene defects are nowadays rare and may only be observed within a single family.[6] To enhance the identification of these rare gene defects researchers gather large IRD cohorts, often use collaborative platforms and tools such as GeneMatcher[36] (https://genematcher.org), and/or engage in collaborations, such as the European Retinal Disease Consortium (ERDC) (http://www.erdc.info/). These resources facilitate the identification of additional cases that provide further evidence supporting the involvement of a newly identified candidate gene. In silico predictions, as well as in vitro and in vivo modeling, may also be valuable approaches to assess the pathogenicity of a novel putative disease-causing gene defect.

Although identifying the gene defect of our initial case (CIC03225) with RCD and macular atrophy was laborious, only WGS in combination with expression data, in silico predictions, and functional analyses highlighted the candidate gene defect. This resulted in a homozygous splice site change in *UBAP1L*, most likely leading to an altered protein length, with a truncated SOUBA domain. Interestingly, we identified 3

additional cases with *UBAP1L* variants through direct Sanger and targeted NGS, in which the UBAP1L protein is predicted to have shorter or absent SOUBA domains or is not functional. This was only possible while screening a large IRD cohort encompassing ~4000 deeply phenotypically and genetically explored index cases with RCD or CRD. Altogether, *UBAP1L* disease-causing variants remain rare in our cohort, with an estimated prevalence of about 0.1%. Of note, the 4 cases identified herein are all originating from consanguineous Tunisian couples with one recurrent variant (ie, NM_001163692.2:c.634_644del) in 2 presumably unrelated families. The prevalence of Tunisian ancestry cases with progressive RCD or CRD in our cohort is unknown. In addition, an *UBAP1L* variant was listed as a potential cause of RP originating from South Asia.[34] It will be interesting, to determine the prevalence of *UBAP1L* variants in Tunisian and other progressive IRD cohorts of different ethnicities.

Regarding the phenotype of the subjects reported herein, 1 case reported primary onset of rod-related symptoms, consistent with the diagnosis of RCD, whereas the other subjects had decreased central vision and abnormal light sensitivity at the onset of symptoms more in line with CRD. Typically, RCD is characterized by primary rod photoreceptor leading to decreased vision in dim light conditions and secondary cone dysfunction and degeneration, usually starting from the peripheral retina, leading to progressive visual-field constriction in day light, typically preserving central vision until late in the course of the disease. On the other hand, CRD usually starts by decreased central vision color-vision defect, light sensitivity, and secondary rod degeneration manifesting with secondary night blindness. The distinction between RCD and CRD dystrophy relies on the patient's visual symptoms, functional tests, such as ff-ERG, which typically show predominant rod dysfunction in case of RCD or cone dysfunction in case of CRD, and multimodal retinal imaging showing predominant peripheral disease and relatively preserved macula in RCD, whereas CRD may display significant macular changes early on in the course of the disease. Nevertheless, the distinction between RCD and CRD may be difficult especially in advanced cases where ff-ERG responses are usually undetectable and somewhat artificial some dystrophies where both photoreceptor systems may appear concomitantly affected. Noticeably, the RCD case from this study (CIC03225) already displayed severe involvement of the central macular region when he was 23 years old, unlike typical RCD cases where the macular region is preserved at the time of presentation. *UBAP1L*-disease-causing variants may therefore be associated with a phenotypic spectrum ranging from RCD with early onset macular involvement to CRD.

Expression analyses using publicly available databases, including Chip-seq data, as well as expression studies on human-derived ROs, RPE cells, and zebrafish collected further evidence for *UBAP1L* to be an excellent candidate gene underlying rod and cone photoreceptor disease.

UBAP1L, is a fairly unknown protein. It is predicted to enable ubiquitin binding activity and is believed to be involved in the ubiquitin-dependent protein catabolic process through the multivesicular body sorting pathway. It is also predicted to be part of endosomal sorting complexes required for transport (ESCRT I complex [https://www.alliancegenome.org/gene/HGNC:40028]). UBAP1L contains a SOUBA domain, which begins at amino acid residue 269 and extends to the C terminus of the protein. This domain is similar to the one found in UBAP1, where it is known to interact with ubiquitin.[35] The role of the N-terminal part of the protein is unknown. The previously reported candidate variant in *UBAP1L*, NM_001163692.2:c.121-2A>C was predicted to lead to exon 3 skipping and an in-frame deletion, p.(His41_Ala233del),[34] which would not affect the SOUBA domain. However, it is predicted to delete a significant portion of the protein and thus leads most likely to a non-functional protein.

In all affected subjects described so far, the SOUBA domain of UBAP1L may be truncated or the protein will be non-functional or absent; thus, ubiquitin binding will not correctly occur. This implies that the ubiquitin proteasome system (UPS) will be altered. The UPS plays an important role in removing abnormal proteins and preventing accumulation of non-functional and harmful proteins within the neuron. Different studies highlighted UPS in retinal health and disease (reviewed in[37]). More specifically, an impairment of the UPS has been associated with pathogenic mechanisms of IRD associated with variants in *RHO* (HGNC:10012),[38] *TOPORS* (HGNC:21653)[39] or *KLHL7* (HGNC:15646)[40] among others. Although variants in these genes have been mainly associated with autosomal dominant IRD and increased ubiquitination, *UBAP1L* variants associated with autosomal recessive IRD leading to truncated SOUBA proteins may induce a dysregulation of the UPS, resulting in cellular stress and photoreceptor degeneration. Functional studies, such as those using mutant and CRISPR/Cas9-edited hiPSCs differentiated in ROs and RPE cells, and zebrafish disease modeling, will be important for further deciphering the pathogenic mechanism implications in *UBAP1L*-associated retinal disorders.

## Data Availability

All data and materials will be supplied upon request.

## Acknowledgments

The authors are thankful to the patient and family members participating in the study and clinical staff from the Reference Center for rare diseases REFERET at Quinze-Vingts hospital. DNA samples included in this study originate from NeuroSensCol DNA bank (PI: JA Sahel, coPI I Audo, partner with Centre Hospitalier National d'Ophtalmologie des Quinze-Vingts, INSERM and CNRS). We thank Maia Brunstein and Beatrix Meha of the Hearing Institute Bioimaging Core Facility of C2RT/C2RA (Institut de l'Audition-Institut Pasteur, Paris, France) for technical support.

## Funding

This research was funded by Fondation Voir et Entendre (C.Z.), by French state funds managed by the Agence Nationale de la Recherche within the Investissements d'Avenir program (ANR-11-IDEX-0004-0), IHU FORe-SIGHT (ANR-18-IAHU-0001 to I.A. and C.Z.) and (ANR-18-IAHU-01 to F.D.B.), Agence Nationale de la Recherche (ANR-18-CE16-0017-01 IPOGUT, ANR-20-CE17-0020-02 INCEPTION, ANR-22-CE17-028 PEMGeT to F.D.B. and ANR-23-CE17-0014-01 RP_SOLVEANDCURE to C.Z., I.A., and F.D.B.), LABEX LIFESENSES (ANR-10-LABX-65 to I.A. and C.Z.) and Fondation pour la Recherche Médicale (MND202003011485 to F.D.B.), Retina France (I.A., C.Z. and F.D.B.), Foundation Fighting Blindness center grant (C-CMM-0907-0428-INSERM04 to I.A. and C.Z.), grant (BR-GE-0619-0761-INSERM to I.A. and C.Z.), UNADEV (Union Nationale des Aveugles et Déficients Visuels to I.A. and C.Z.) in partnership with ITMO NNP/AVIESAN (alliance nationale pour les sciences de la vie et de la santé) for research in visual disorders, and doctoral funding from the Ministère de l'Enseignement Supérieur et de la Recherche (MESR) and Fondation de France (C.M. and J.W.).

## Author Information

Conceptualization: C.Z., I.A.; Data Curation: J.N., L.A.P., C.M., L.M.N., C.C., A.Antonio, C.L., T.B.-Y., J.W., C.A., L.B., A.Antropoli, M.N., S.E.S., V.S., S.C.-B., S.M.-S., I.A., J.-A.S., M.S., A.Amprou, S.A.; Formal Analysis: J.N., L.A.P., C.M., L.M.N., C.C., A.Antonio, C.L., C.A., L.B., A.Antropoli, M.N., S.E.S., V.S., S.C.-B., S.M.-S., I.A., M.S., S.A.; Supervision: C.Z., I.A., F.D.B., S.A.; Funding Acquisition: J.A.-S., C.Z., I.A., F.D.B.; Writing-original draft: C.Z., I.A.; Writing-review and editing: J.N., S.A., F.D.B.

## Ethics Declaration

Written informed consent was obtained from all individuals. All studies were carried out in accordance with the declaration of Helsinki and were approved by a national ethics committee (CPP Ile de France V, Project number 06693, N∘EUDRACT 2006-A00347-44, 11 December 2006).

## Conflict of Interest

The authors declare no conflicts of interest.

## Additional Information

The online version of this article (https://doi.org/10.1016/j.gim.2024.101081) contains supplemental material, which is available to authorized users.

## Affiliations

[1]Sorbonne Université, INSERM, CNRS, Institut de la Vision, Paris, France; [2]Mass. Eye and Ear, Ocular Genomics Institute, Berman-Gund Laboratory for the Study of Retinal Degenerations, Harvard Medical School, Boston, MA; [3]UCL Institute of Ophthalmology, London, UK; [4]The Francis Crick Institute, London, UK; [5]Instituto Nacional de Saúde da Mulher, da Criança e do Adolescente Fernandes Figueira, Fundação Oswaldo Cruz, Rio de Janeiro, Brazil; [6]Department of Biological Structure, University of Washington, Seattle, WA; [7]Centre Hospitalier National d'Ophtalmologie des Quinze-Vingts, Centre de Référence Maladies Rares REFERET and INSERM-DGOS CIC 1423, Paris, France; [8]Department of Ophthalmology, IRCCS San Raffaele Scientific Institute, Milan, Italy; [9]Department of Clinical Sciences and Community Health, University of Milan, Milan, Italy; [10]Molecular Testing Laboratory, Department of Medical Laboratory Technology, Faculty of Health Sciences, Beirut Arab University, Beirut, Lebanon; [11]APHP, Hôpital Armand-Trousseau, Département de Génétique, UF de Génétique Chromosomique, Paris, France; [12]Exploration de la Vision et Neuro-Ophtalmologie, CHU de Lille, Lille, France; [13]Department of Ophthalmology, The University of Pittsburgh School of Medicine, Pittsburgh, PA

## References

1. Lindsay S, Inglehearn CF, Curtis A, Bhattacharya S. Molecular genetics of inherited retinal degenerations. *Curr Opin Genet Dev*. 1992;2(3):459-466. http://doi.org/10.1016/s0959-437x(05)80158-3
2. Hamel C. Retinitis pigmentosa. *Orphanet J Rare Dis*. 2006;1:40. http://doi.org/10.1186/1750-1172-1-40
3. Roosing S, Thiadens AA, Hoyng CB, Klaver CC, den Hollander AI, Cremers FP. Causes and consequences of inherited cone disorders. *Prog Retin Eye Res*. 2014;42:1-26. http://doi.org/10.1016/j.preteyeres.2014.05.001
4. Berger W, Kloeckener-Gruissem B, Neidhardt J. The molecular basis of human retinal and vitreoretinal diseases. *Prog Retin Eye Res*. 2010;29(5):335-375. http://doi.org/10.1016/j.preteyeres.2010.03.004
5. Schneider N, Sundaresan Y, Gopalakrishnan P, et al. Inherited retinal diseases: linking genes, disease-causing variants, and relevant therapeutic modalities. *Prog Retin Eye Res*. 2022;89:101029. http://doi.org/10.1016/j.preteyeres.2021.101029

6. Zeitz C, Méjécase C, Michiels C, et al. Mutated CCDC51 coding for a mitochondrial protein, MITOK is a candidate gene defect for autosomal recessive rod-cone dystrophy. *Int J Mol Sci*. 2021;22(15):7875. http://doi.org/10.3390/ijms22157875
7. Méjécase C, Hummel A, Mohand-Saïd S, et al. Whole exome sequencing resolves complex phenotype and identifies CC2D2A mutations underlying non-syndromic rod-cone dystrophy. *Clin Genet*. 2019;95(2):329-333. http://doi.org/10.1111/cge.13453
8. Solaguren-Beascoa M, Bujakowska KM, Méjécase C, et al. WDR34, a candidate gene for non-syndromic rod-cone dystrophy. *Clin Genet*. 2021;99(2):298-302. http://doi.org/10.1111/cge.13872
9. Zeitz C, Michiels C, Neuillé M, et al. Where are the missing gene defects in inherited retinal disorders? Intronic and synonymous variants contribute at least to 4% of CACNA1F-mediated inherited retinal disorders. *Hum Mutat*. 2019;40(6):765-787. http://doi.org/10.1002/humu.23735
10. Weisschuh N, Buena-Atienza E, Wissinger B. Splicing mutations in inherited retinal diseases. *Prog Retin Eye Res*. 2021;80:100874. http://doi.org/10.1016/j.preteyeres.2020.100874
11. de Bruijn SE, Fiorentino A, Ottaviani D, et al. Structural variants create new topological-associated domains and ectopic retinal enhancer-gene contact in dominant retinitis pigmentosa. *Am J Hum Genet*. 2020;107(5):802-814. http://doi.org/10.1016/j.ajhg.2020.09.002
12. Ueyama H, Li YH, Fu GL, et al. An A-71C substitution in a green gene at the second position in the red/green visual-pigment gene array is associated with deutan color-vision deficiency. *Proc Natl Acad Sci U S A*. 2003;100(6):3357-3362. http://doi.org/10.1073/pnas.0637437100
13. Cremers FPM, Boon CJF, Bujakowska K, Zeitz C. Special issue introduction: inherited retinal disease: novel candidate genes, genotype-phenotype correlations, and inheritance models. *Genes (Basel)*. 2018;9(4):215. http://doi.org/10.3390/genes9040215
14. Biswas P, Borooah S, Matsui H, et al. Detection and validation of novel mutations in MERTK in a simplex case of retinal degeneration using WGS and hiPSC-RPEs model. *Hum Mutat*. 2021;42(2):189-199. http://doi.org/10.1002/humu.24146
15. Audo I, Friedrich A, Mohand-Saïd S, et al. An unusual retinal phenotype associated with a novel mutation in RHO. *Arch Ophthalmol*. 2010;128(8):1036-1045. http://doi.org/10.1001/archophthalmol.2010.162
16. Audo I, Sahel JA, Mohand-Saïd S, et al. EYS is a major gene for rod-cone dystrophies in France. *Hum Mutat*. 2010;31(5):E1406-E1435. http://doi.org/10.1002/humu.21249
17. Audo I, Lancelot ME, Mohand-Saïd S, et al. Novel C2orf71 mutations account for ~1% of cases in a large French arRP cohort. *Hum Mutat*. 2011;32(4):E2091-E2103. http://doi.org/10.1002/humu.21460
18. Ávila-Fernández A, Cantalapiedra D, Aller E, et al. Mutation analysis of 272 Spanish families affected by autosomal recessive retinitis pigmentosa using a genotyping microarray. *Mol Vis*. 2010;16:2550-2558.
19. Audo I, Bujakowska KM, Léveillard T, et al. Development and application of a next-generation-sequencing (NGS) approach to detect known and novel gene defects underlying retinal diseases. *Orphanet J Rare Dis*. 2012;7(1):8. http://doi.org/10.1186/1750-1172-7-8
20. Boulanger-Scemama E, El Shamieh S, Démontant V, et al. Next-generation sequencing applied to a large French cone and cone-rod dystrophy cohort: mutation spectrum and new genotype-phenotype correlation. *Orphanet J Rare Dis*. 2015;10:85. http://doi.org/10.1186/s13023-015-0300-3
21. Marchal C, Singh N, Batz Z, et al. High-resolution genome topology of human retina uncovers super enhancer-promoter interactions at tissue-specific and multifactorial disease loci. *Nat Commun*. 2022;13(1):5827. http://doi.org/10.1038/s41467-022-33427-1
22. Cherry TJ, Yang MG, Harmin DA, et al. Mapping the cis-regulatory architecture of the human retina reveals noncoding genetic variation in disease. *Proc Natl Acad Sci U S A*. 2020;117(16):9001-9012. http://doi.org/10.1073/pnas.1922501117
23. El Shamieh S, Neuillé M, Terray A, et al. Whole-exome sequencing identifies KIZ as a ciliary gene associated with autosomal-recessive rod-cone dystrophy. *Am J Hum Genet*. 2014;94(4):625-633. http://doi.org/10.1016/j.ajhg.2014.03.005
24. Jaganathan K, Kyriazopoulou Panagiotopoulou S, McRae JF, et al. Predicting splicing from primary sequence with deep learning. *Cell*. 2019;176(3):535-548.e24. http://doi.org/10.1016/j.cell.2018.12.015
25. Zeng T, Li YI. Predicting RNA splicing from DNA sequence using Pangolin. *Genome Biol*. 2022;23(1):103. http://doi.org/10.1186/s13059-022-02664-4
26. Quinodoz M, Peter VG, Bedoni N, et al. AutoMap is a high performance homozygosity mapping tool using next-generation sequencing data. *Nat Commun*. 2021;12(1):518. http://doi.org/10.1038/s41467-020-20584-4
27. Terray A, Slembrouck A, Nanteau C, et al. Generation of an induced pluripotent stem cell (iPSC) line from a patient with autosomal dominant retinitis pigmentosa due to a mutation in the NR2E3 gene. *Stem Cell Res*. 2017;24:1-4. http://doi.org/10.1016/j.scr.2017.08.003
28. Reichman S, Slembrouck A, Gagliardi G, et al. Generation of storable retinal organoids and retinal pigmented epithelium from adherent human iPS cells in xeno-free and feeder-free conditions. *Stem Cells*. 2017;35(5):1176-1188. http://doi.org/10.1002/stem.2586
29. Wohlschlegel J, Letellier C, Liu B, et al. Generation of human induced pluripotent stem cell lines from a patient with ITM2B-related retinal dystrophy and a non mutated brother. *Stem Cell Res*. 2019;41:101625. http://doi.org/10.1016/j.scr.2019.101625
30. Orozco LD, Chen HH, Cox C, et al. Integration of eQTL and a single-cell atlas in the human eye identifies causal genes for age-related macular degeneration. *Cell Rep*. 2023;42(3):112298. http://doi.org/10.1016/j.celrep.2023.112298
31. Rosello M, Vougny J, Czarny F, et al. Precise base editing for the in vivo study of developmental signaling and human pathologies in zebrafish. *eLife*. 2021;10:e65552. http://doi.org/10.7554/eLife.65552
32. Oxtoby E, Jowett T. Cloning of the zebrafish krox-20 gene (krx-20) and its expression during hindbrain development. *Nucleic Acids Res*. 1993;21(5):1087-1095. http://doi.org/10.1093/nar/21.5.1087
33. Jumper J, Evans R, Pritzel A, et al. Highly accurate protein structure prediction with AlphaFold. *Nature*. 2021;596(7873):583-589. http://doi.org/10.1038/s41586-021-03819-2
34. Carss KJ, Arno G, Erwood M, et al. Comprehensive rare variant analysis via whole-genome sequencing to determine the molecular pathology of inherited retinal disease. *Am J Hum Genet*. 2017;100(1):75-90. http://doi.org/10.1016/j.ajhg.2016.12.003
35. Agromayor M, Soler N, Caballe A, et al. The UBAP1 subunit of ESCRT-I interacts with ubiquitin via a SOUBA domain. *Structure*. 2012;20(3):414-428. http://doi.org/10.1016/j.str.2011.12.013
36. Sobreira N, Schiettecatte F, Valle D, Hamosh A. GeneMatcher: a matching tool for connecting investigators with an interest in the same gene. *Hum Mutat*. 2015;36(10):928-930. http://doi.org/10.1002/humu.22844
37. Campello L, Esteve-Rudd J, Cuenca N, Martín-Nieto J. The ubiquitin-proteasome system in retinal health and disease. *Mol Neurobiol*. 2013;47(2):790-810. http://doi.org/10.1007/s12035-012-8391-5
38. Illing ME, Rajan RS, Bence NF, Kopito RR. A rhodopsin mutant linked to autosomal dominant retinitis pigmentosa is prone to aggregate and interacts with the ubiquitin proteasome system. *J Biol Chem*. 2002;277(37):34150-34160. http://doi.org/10.1074/jbc.M204955200
39. Czub B, Shah AZ, Alfano G, Kruczek PM, Chakarova CF, Bhattacharya SS. TOPORS, a dual E3 ubiquitin and Sumo1 ligase, interacts with 26 S protease regulatory Subunit 4, encoded by the PSMC1 gene. *PLoS One*. 2016;11(2):e0148678. http://doi.org/10.1371/journal.pone.0148678
40. Kim J, Tsuruta F, Okajima T, Yano S, Sato B, Chiba T. KLHL7 promotes TUT1 ubiquitination associated with nucleolar integrity: implications for retinitis pigmentosa. *Biochem Biophys Res Commun*. 2017;494(1-2):220-226. http://doi.org/10.1016/j.bbrc.2017.10.049